Major Article

Interactions between Severe Acute Respiratory Syndrome Coronavirus 2 Replication and Major Respiratory Viruses in Human nasal Epithelium

Pizzorno Andrés[1], Padey Blandine[1,2], Dulière Victoria[1,4], Mouton William[1,3], Oliva Justine[1], Emilie Laurent[1,4], Milesi Cedrine[1], Lina Bruno[1], Traversier Aurelien[1,4], Julien Thomas[1,4], Trouillet-Assant Sophie[1,3], Rosa-Calatrava Manuel[1,4*], Terrier Olivier[1*#]

1. CIRI, Centre International de Recherche en Infectiologie, (Team VirPath), Univ Lyon, Inserm, U1111, Université Claude Bernard Lyon 1, CNRS, UMR5308, ENS de Lyon, F-69007, Lyon, France.

2. Signia Therapeutics SAS, Lyon, France.

3. Laboratoire Commun de Recherche, Hospices Civils de Lyon, bioMérieux, Centre Hospitalier Lyon Sud, Pierre-Bénite, France.

4. VirNext, Faculté de Médecine RTH Laennec, Université Claude Bernard Lyon 1, Université de Lyon, Lyon, France.

*RCM & TO are co-last authors

Correspondence to: Olivier Terrier. CIRI, Centre International de Recherche en Infectiologie, (Team VirPath), Univ Lyon, Inserm, U1111, Université Claude Bernard Lyon 1, CNRS, UMR5308, ENS de Lyon, F-69007, Lyon, France, (olivier.terrier@univ-lyon1.fr)

Abstract

The emergence of severe acute respiratory syndrome coronavirus 2 (SARS-CoV-2), along with extensive non-pharmacological interventions, have profoundly altered the epidemiology of major respiratory viruses. Some studies have described virus-virus interactions, particularly manifested by viral interference mechanisms at different scales. Still, our knowledge of the mutual interactions between SARS-CoV-2 and other respiratory viruses remains incomplete. Here, we studied the interactions between SARS-CoV-2 and several respiratory viruses (influenza, RSV, hMPV, and hRV) in a reconstituted human epithelial airway model, exploring different scenarios affecting the sequence and timing of co-infections. We show that the virus type and the sequence of infections are key parameters of virus-virus interactions, having the impact of primary infections on the regulation of the immune response a determinant role in the outcome of secondary infections.

Keywords

SARS-CoV-2; virus-virus interactions; influenza virus; Respiratory syncytial virus; Human Rhinovirus; Human Metapneumovirus

Running Title

SARS-CoV-2 respiratory viral coinfections

INTRODUCTION

The emergence of SARS-CoV-2 in late 2019 and the consequent COVID-19 pandemic had, and still have, a massive impact on our societies. Beyond the more than 526 million confirmed cases and over 6.28 million deaths [1], multivariate estimates point to over 40% of the global population having been infected at least once before the recent rising of the SARS-CoV-2 omicron variant [2]. The magnitude of the health crisis has somewhat overshadowed the contribution of acute respiratory infections to global mortality, which are responsible for 3 to 5 million deaths per year in non-pandemic periods [3]. Several studies have shown that the global circulation of SARS-CoV-2 has profoundly altered the epidemiological pattern of the main respiratory viruses, such as influenza viruses and Respiratory Syncytial Virus (RSV) [4]. Early in 2020, many countries implemented non-pharmaceutical interventions (e.g., face masks, social distancing, lockdown, school closures, or teleworking) and travel restrictions to mitigate the transmission of SARS-CoV-2 and subsequently saw a rapid decline in influenza infections, with influenza circulation in the northern hemisphere at an all-time low despite higher numbers of specimens tested [4–7]. At the same time, a shift on RSV outbreaks, occurring at unusual times of the year, has been observed [8–10]. Although other mechanisms for the predominance of SARS-CoV-2 cannot be excluded (e.g., underestimation/detection/reporting of other respiratory viruses, more limited access to treatment of other respiratory infections, competitive interference), health restrictions seem to have played a major role, as suggested by recent reports showing significant increases in the circulation of influenza and other respiratory viruses concomitantly with the ease of restrictions [11,12].

There is relatively little information on the severity of COVID-19 in the context of co-infection with other viruses, apart from a few studies involving a small number of patients,

some of which suggest a possible deleterious effect [13–16]. The simultaneous circulation of different viruses can give rise to synergistic, neutral, or antagonistic interactions, ranging from the local environment of the respiratory epithelial cell to a population epidemic dynamics level [17]. Competitive interference has been described in the case of co-circulation between respiratory viruses, notably involving influenza viruses. However, there is still no clear consensus about the consequences of these co-infections in terms of disease severity [18,19]. *In vitro* approaches have shown, for example, that RSV growth is blocked by competitive infection with influenza A virus [20] or that primary viral infection with a rhinovirus reduces replication of subsequent influenza infection [21,22]. The underlying mechanisms are not yet fully understood and would involve viral competition for host resources but also the induction of temporary non-specific host immunity [19,21,22].

Several teams have tried to address these questions concerning the potential interactions between SARS-CoV-2 and other respiratory viruses, with relatively similar experimental designs and observations. They have notably shown that primary infection with rhinovirus prevents secondary infection with SARS-CoV-2 [23–26]. Fage and colleagues recently showed that prior infection of human epithelial cells with SARS-CoV-2 interferes with the replication kinetics of H1N1 influenza virus and RSV, while only H1N1 infection reduces subsequent SARS-CoV-2 infection [27]. Cheemarla and collaborators have notably shown that the activity of Interferon-Stimulated Genes-mediated response at the time of SARS-CoV-2 exposure impacts infection progression [24]. Altogether, these studies suggest a prominent role for the innate immune response in these virus-virus interactions, at least when co-infections are very close in time. Nevertheless, our knowledge of the mutual interactions between SARS-COV-2 and respiratory viruses remains incomplete.

In this study, we aimed to further explore the interactions between SARS-CoV-2 and several respiratory viruses, such as influenza viruses, RSV, hMPV, or hRV using a reconstituted

human airway epithelium model (HAE). We studied and compared the mutual impacts on viral replication, epithelial integrity, but also innate immune signatures in different infection and superinfection scenarios. Our results suggest that the timing, sequence, and specific nature of the induced immune response are key elements in the interactions between SARS-CoV-2 and other viruses.

METHODS

Viral strains

All experiments involving clinical samples and the manipulation of infectious SARS-CoV-2 were performed in biosafety level 3 (BSL-3) facilities, using appropriate protocols. The SARS-CoV-2 strain used in this study (BetaCoV/France/IDF0571/2020; GISAID accession ID EPI_ISL_411218) is a Wuhan-Like B strain isolated from a nasal swab sample collected from a one of the first COVID-19 cases confirmed in France [28]. Rhinovirus A16 (hRV-A16 ATCC VR-283) was a king gift from Samuel Constant (Epithelix SARL). Influenza A/Lyon/969/2009(H1N1), Respiratory syncytial virus (hRSV-A Long strain ATCC-VR26) and human metapneumovirus (hMPV-B strain CAN97-82 (B1)) were previously described [29]. All these viruses were produced and titrated in dedicated cell lines, and the replication kinetics of each strain in the HAE model were previously performed [28,29].

Viral infections in reconstituted human airway epithelia (HAE)

Infections protocols in HAE were previously described [28,29]. Briefly, MucilAir^{TM} HAE reconstituted from human primary cells obtained from nasal biopsies, were provided by Epithelix SARL (Geneva, Switzerland) and maintained in air-liquid interphase with specific

culture medium in Costar Transwell inserts (Corning, NY, USA) according to the manufacturer's instructions. For infection experiments, apical poles were gently washed twice with warm OptiMEM medium (Gibco, ThermoFisher Scientific) and then infected directly with 150 µl of calibrated viral suspension in OptiMEM medium, at a specific multiplicity of infection (MOI). For mock infection, the same procedure was followed using OptiMEM as inoculum. Transepithelial electrical resistance (TEER) was measured using a dedicated volt-ohm meter (EVOM2, Epithelial Volt/Ohm Meter for TEER) and expressed as $Ohm.cm^2$.

Transmission electron microscopy

Infected nasal HAE were fixed with 2% glutaraldehyde (EMS) in 0.1 M sodium cacodylate (pH 7.4) buffer at room temperature for 30 min. After washing three times in 0.2 M sodium cacodylate buffer, cell cultures were post-fixed with 2% osmium tetroxide (EMS) at room temperature for 1 h and dehydrated in a graded series of ethanol at room temperature and embedded in Epon. After polymerization, ultrathin sections (100 nm) were cut on a UCT (Leica) ultramicrotome and collected on 200 mesh grids. Sections were stained with uranyl acetate and lead citrate before observations on a Jeol 1400JEM (Tokyo, Japan) transmission electron microscope, equipped with an Orius 600 camera and Digital Micrograph Software (Gatan).

Real-time quantitative PCR

Relative quantification of viral genome was performed by one-step real-time quantitative reverse transcriptase and polymerase chain reaction (RT-qPCR) from viral or total RNA extracted using QiAmp viral RNA or RNeasy Mini Kit (Qiagen) in the case of supernatants/apical washings or cell lysates, respectively. The relative quantification of the

viral genes was performed by RTqPCR or SYBR-Green using the StepOnePlus™ Real-Time PCR System (Applied Biosystems) in 96-well plates. Each sample was analyzed in triplicate, and the cycle threshold (Ct) values were normalized against the endogenous GAPDH reference, when necessary. The primers and probes used are described in Table 1.

Nanostring gene expression analysis

The NanoString nCounter® technology, a hybridization-based multiplex assay characterized by its amplification-free step, was used for mRNA detection of two customized panels: "immune response" (96 genes) and "type III IFNs" (12 genes) [28]. Data treatment and normalization were next performed using nSolver analysis software (version 4.0, NanoString technologies). A first step of normalization using the internal positive controls allowed correction of a potential source of variation associated with the technical platform. To normalize for differences in RNA input we used the same method as in the positive control normalization, except that geometric means were calculated over several housekeeping genes. After normalization steps, the ratio between infected/co-infected condition and the mock condition were calculated to compare gene expression. Results were expressed as fold change induction. Heatmaps were generated using Morpheus (Broad Institute, Morpheus, https://software.broadinstitute.org/morpheus).

RESULTS

Simultaneous influenza virus and SARS-CoV-2 infections

Based on protocols previously described [28,29], we initially performed single infections or co-infection with H1N1 influenza virus (H1N1pdm09) and/or SARS-CoV-2 (B, Wuhan-like strain) in a HAE model of nasal origin. Infections/co-infections were performed at a MOI of 1 and monitored over a 48-hour period (Figure 1A). As expected, single infections strongly

impact epithelial integrity at 48 hpi, with a 40-80% decrease in trans-epithelial resistance (TEER ohms.cm2) values for H1N1 and SARS-CoV-2, respectively. Such deleterious impact of co-infection on epithelium integrity was comparable to that observed in the case of single infection with SARS-CoV-2 (Figure 1B). In terms of viral replication, we found a very modest decrease in normalized intracellular SARS-CoV-2 genome levels between single infection and co-infection (18%, nsp14/GAPDH, Figure 1C), whereas this difference was much greater in the case of H1N1 (74%, M/GADPH, Figure 1D). Observation of the different experimental conditions by electron microscopy (Figure 1E) shows characteristic signs of infection with SARS-CoV-2 (Figure 1E, panel b) or H1N1 (Figure 1E, panel c). In the case of co-infection, these same characteristics are found on neighboring cells (Figure 1E, panel D), but rarely within the same cell. Altogether, our initial observations suggest a mutual antagonism of the two viruses yet with differential amplitude in HAE model.

Influenza and SARS-CoV-2 mutual superinfections

We then performed mutual superinfection experiments in HAE, in which a primary viral infection with one of the viruses (MOI 0.1) was followed by a secondary infection with the other virus (MOI 0.1) 48h later. The final readout was fixed at 96hpi, namely 48h post superinfection (Figure 2A). Under these conditions, single infection with influenza virus induces a marked (>50%) drop in TEER values at 48hpi and to a lesser extent at 96hpi. Single SARS-CoV-2 infection induced a comparable decrease at 48hpi though TEER values remained low at 96hpi (Figure 2B). In the case of superinfections, TEER values followed the same pattern observed for single infections with the primary virus, suggesting no or minor supplementary impact of the viral superinfection on the integrity of the respiratory epithelium at 96 hpi (Figure 2B). We then quantified for each condition the viral genome of both viruses at the apical region of the HAE (Figure 2C) and also at the intracellular level (Figure 2D).

While SARS-CoV-2 superinfection 48h after a primary influenza infection does not significantly alter influenza M gene copy levels either at the apical or intracellular level, the opposite sequence of superinfection (i.e. H1N1 superinfection following primary SARS-CoV-2 infection) appears to marginally reduce apical SARS-CoV-2 nsp14 gene copy levels (Figure 2C/D). These results are in line with previous TEER observations suggesting a minimal level of interference during viral superinfection in HAE model.

To complete our investigations, we used the nanostring technology to study the expression of a wide panel of genes involved in the host innate immune response at 96hpi (Figure 2E). Interestingly, the comparison of the immune signatures of superinfections with those of the corresponding single infections reflect quite different profiles for influenza virus or SARS-CoV-2. Indeed, compared to the condition of simple influenza infection, we observe a significant upregulation of a large proportion of the genes in the panel during superinfection with SARS-CoV-2, with the notable exception of several genes (IL1A, IL1B, IL1R2, FAM89A, PTGS2, IL7R, MIP2α, IL18, and IL6) which are mainly involved in the inflammatory response (orange box, Figure 2E). In contrast, several genes involved in the early interferon-stimulated innate immune response (OAS1, OAS2, SOCS1, DDX58, CXCL10) are upregulated following influenza superinfection when compared to corresponding SARS-CoV-2 simple infection (green boxes, Figure 2E). Overall, these observations suggest that the sequential order of superinfection is crucial for the differential regulation of early host immune and inflammatory responses.

SARS-CoV-2 delayed superinfection following an influenza, RSV, hMPV or hRV primo-infection

As the experimental co-infection and superinfection protocols described above do not necessarily fully reflect the different interaction scenarios found in patients, we finally sought

to mimic a situation of delayed superinfection by SARS-CoV-2 in the context of a primary infection by influenza but also by other major respiratory viruses, such as Respiratory Syncytial Virus (RSV), Human Metapneumovirus (hMPV) or Human Rhinoviruses (hRV). For this, we performed primary infections with H1N1 (MOI 0.01), RSV (MOI 0.1), hMPV (MOI 1) and hRV (MOI 5) in HAE and followed by superinfection with SARS-CoV-2 (MOI 0.1) at 7dpi, with final readout 48h later (9dpi) (Figure 3A). As expected, primary influenza, RSV and hMPV infections had a deleterious impact on epithelial integrity, with the greatest decreases on TEER values observed for H1N1 and RSV at 7 and 9dpi. No significant effect of Rhinovirus infection on TEER was observed (Figure 3B). Similar to our previous observations, we did not observe any additional effect of SARS-CoV-2 superinfection on epithelium integrity at 9dpi (Figure 3B). Furthermore, superinfection with SARS-CoV-2 had no significant impact on the intracellular genome levels of influenza, hMPV and hRV, with only a 2-fold reduction in the context of primary RSV infection (Figure 3C).

On the other hand, SARS-CoV-2 nsp14 gene copy levels at 9dpi (48h post SARS-CoV-2 infection or superinfection) were significantly lower in the context of primary influenza, RSV, and hMPV viral infections than in the mock primo-infected condition, hence suggesting very strong viral interference in HAE model. This effect was much less pronounced in the context of hRV primoinfection (Figure 3D). These observations are in line with the immune signatures determined by nanostring (Figure 4). We have plotted the deregulation of gene expression during SARS-CoV-2 superinfection against the level of expression measured during primary infection (Superinf. H1N1, hRSV, hMPV & hRV, Figure 4 & Supplementary Figure 1). This heatmap visualization reflects quite well the very strong interference of primary viral infection, despite a long infection time, and illustrates the similarities and differences between each viral model. Indeed, there is a clear clustering between H1N1/hRSV and hMPV/hRV SARS-CoV-2 superinfections, with the regulation of genes such as IL18,

IL1A, IRF3, JAK2 being particularly discriminating, with down- or up-regulation, respectively (yellow box, Figure 4). Some gene clusters are deregulated in a way that is very specific to the nature of the primary infection, for example the downregulation of ZBTB16, TBP, EI2AK4, DECTIN-1, POU2F2, IL7R is very specific to the RSV+SARS-CoV-2 superinfection (green box, Figure 4). Similarly, the upregulation of a very large number of genes, including CXCL10, OAS1/OAS2, IRAK2, STAT2, IFI44L, MX1, IFITM1 or IFI35, seems characteristic of hRV+SARS-COV-2 superinfection (orange boxes, Figure 4) and suggests a more pronounced level of interference than for the other viruses studied, under these experimental conditions. Altogether, these observations show that the nature of the primary infection is an important driver in the host response.

DISCUSSION

After two years of an ongoing pandemic and the gradual lifting of sanitary restrictions in many countries, we now find ourselves in a rather unprecedented situation, with the co-circulation of SARS-CoV-2 with other main respiratory viruses. This situation raises many questions about the mechanisms of interaction between these different viruses, but also about the consequences of these co-infections/superinfection and their clinical management. In this study, we aimed to further explore the interactions between SARS-CoV-2 and several respiratory viruses, such as influenza viruses, RSV, hMPV, or hRV using a reconstituted HAE model. This model, consisting of human airway primary cells grown at the air/liquid interface, is a truly relevant model for studying respiratory viruses and within-host interactions. For example, our group has used this model several times to characterize and compare different respiratory viruses such as influenza viruses, RSV, hMPV [29,34] or

SARS-CoV-2 [28], but also to experimentally simulate scenarios of interactions between pathogens, including bacterial/fungal superinfections [35–37].

One of our first observations showed a reciprocal deleterious impact between influenza viruses and SARS-CoV-2 in the context of simultaneous infection (Figure 1). Although this experimental scheme might be uncommon in the context of natural infections, it allowed us to show that simultaneous infection of the HAE model by viruses using distinct receptors and entry pathways was possible, but also that the reciprocal impact between viruses was not necessarily of the same order. Our results do indeed show a much greater impact of SARS-CoV-2 on influenza than vice versa, but it is very difficult to know whether this reflects a characteristic of SARS-CoV-2 or simply a difference due to a distinct infectivity or greater replication. We then chose to explore models of superinfection, prioritizing sufficiently large time gaps between primary and secondary infection to allow for multi-cycle replication and significant host response to the infections. While many studies have examined the effect of a pre-existing infection on the outcome of the second infection, in one direction only, it is extremely instructive to be able to compare the mirror-image superinfection scenarios. In a context of successive infections with a 48-hour delay, we showed that SARS-CoV-2 infection is slightly reduced by superinfection with H1N1, which is not the case in the reverse situation (Figure 2). In a context of successive infections with a much longer delay (7 days), we showed that superinfection with SARS-CoV-2 had no significant impact on primary infections, except for RSV. Under the same conditions, we also found that primary viral infections induced an unfavorable state for SARS-CoV-2 replication, with significant differences for some viruses – hRV being the less impactful (Figure 3). These results are in a relatively good agreement with the work previously published by Essaidi-Laziozi &

colleagues [25] and only partially with those obtained by Fage & colleagues [27], which can probably be explained by differences in protocols and experimental parameters.

The comparison of immune signatures between simple infections and superinfections allowed us to highlight specificities linked to the sequential order of the infections. While a superinfection with influenza virus in the context of a primary SARS-COV-2 infection manifests itself by a rather characteristic antiviral signature (Figure 2E), the opposite scenario results in an inflammatory signature which suggests a more severe context when SARS-CoV-2 is the second pathogen. Although primary viral infections provide varying degrees of control of secondary infection with SARS-CoV-2, the nature of the resulting immune response may be distinct for different combinations of pathogens and may constitute a more or less favorable terrain for disease progression. Our results in HAE model are in line with *in vivo* studies that showed that greater severity was associated with SARS-CoV-2 superinfection. For example, Kim and colleagues showed that SARS-CoV-2/influenza virus coinfections in K18-ACE2 mice caused an unbalanced immune response in the lungs and peripheral blood, with more pronounced lung damage and longer secondary infections [38]. In another model, (golden Syrian hamster), it was recently shown that simultaneous or sequential co-infection with SARS-CoV-2 and H1N1 induced more severe disease than single infection with either virus. Interestingly, prior infection with H1N1 virus reduced the pulmonary viral load of SARS-CoV-2 but increased lung damage [39], in line with the enhanced inflammatory expression profile observed in the context of H1N1+SARS-CoV-2 superinfections in our study (Figure 2).

Although our results and those available in the literature indicate quite clearly the importance of the IFN response in SARS-CoV-2/respiratory virus interactions, with differences specific

to each virus, it remains very difficult to really determine whether this is related to intra-specific, virus-specific characteristics or rather to experimental biases. Indeed, as is the case in many studies, particularly the study of *in vitro* interactions between pathogens, the comparison between different viruses as different as influenza, RSV or even SARS-CoV-2, in a given model, is very complex, as very large differences can exist notably in terms of infectivity, delay of the induction of the IFN response, replication kinetics and within-host interaction. Therefore, it is important to multiply the different possible scenarios of co-infection, by playing with the parameters of infection, sequence, and timing of infection when possible. Although the data generated in our experimental models are not the perfect proxy for simulating clinical situations of co-infections, they are nevertheless a very good starting point, complementary to *in vivo* studies, but also mathematical modeling approaches [18] to improve our understanding of the underlying virus-virus interactions. In order to better understand these interactions at the scale of the respiratory epithelium, it will also be necessary to explore the various models set up with much more global approaches, in particular by calling upon "omics" approaches (e.g., transcriptional profiling, metabolomics) in order to have a more complete vision of within-host interactions, beyond the responses involving the immune response.

In this situation of co-circulation of respiratory viruses and SARS-CoV-2, it is essential to continue our efforts to better understand the interactions between these different viruses, at different scales. This knowledge is essential to guide prophylactic and therapeutic approaches in such clinical situations. From this point of view, the development of host-targeted antiviral strategies with broad-spectrum efficacy could strengthen our arsenal to fight coinfections.

NOTES

Acknowledgments

The authors would like to thank all their colleagues in the VirPath team (CIRI, Lyon - France), for their help and useful comments. The Authors also thank Elisabeth Errazuriz Centre d'Imagerie Quantitative Lyon Est (CIQLE) for her precious help with electron microscopy.

Financial support

This work was funded by INSERM REACTing (REsearch & ACtion emergING infectious diseases), CNRS, and Mérieux research grants. This work is in the scope of the French research network on influenza viruses (ResaFlu; GDR2073) financed by the CNRS.

Potential conflicts of interests

The authors declare no conflicts of interest in relation to this study

REFERENCES

1. WHO Coronavirus Disease (COVID-19) Dashboard [Internet]. [cited 2020 May 19]. Available from: https://covid19.who.int/

2. COVID-19 Cumulative Infection Collaborators. Estimating global, regional, and national daily and cumulative infections with SARS-CoV-2 through Nov 14, 2021: a statistical analysis. Lancet. **2022**; :S0140-6736(22)00484–6.

3. WHO | Acute respiratory infections [Internet]. WHO. [cited 2013 Oct 24]. Available from: http://www.who.int/vaccine_research/diseases/ari/en/

4. Kim D, Quinn J, Pinsky B, Shah NH, Brown I. Rates of Co-infection Between SARS-CoV-2 and Other Respiratory Pathogens. JAMA. **2020**; 323(20):2085–2086.

5. Adlhoch C, Pebody R. What to expect for the influenza season 2020/21 with the ongoing COVID-19 pandemic in the World Health Organization European Region. Euro Surveill. **2020**; 25(42):2001816.

6. Larrauri A, Prosenc Trilar K. Preparing for an influenza season 2021/22 with a likely co-circulation of influenza virus and SARS-CoV-2. Euro Surveill. **2021**; 26(41):2100975.

7. Olsen SJ, Azziz-Baumgartner E, Budd AP, et al. Decreased influenza activity during the COVID-19 pandemic-United States, Australia, Chile, and South Africa, 2020. Am J Transplant. **2020**; 20(12):3681–3685.

8. Casalegno J-S, Ploin D, Cantais A, et al. Characteristics of the delayed respiratory syncytial virus epidemic, 2020/2021, Rhône Loire, France. Euro Surveill. **2021**; 26(29).

9. Rybak A, Levy C, Jung C, et al. Delayed Bronchiolitis Epidemic in French Primary Care Setting Driven by Respiratory Syncytial Virus: Preliminary Data from the Oursyn Study, March 2021. Pediatr Infect Dis J. **2021**; 40(12):e511–e514.

10. Weinberger Opek M, Yeshayahu Y, Glatman-Freedman A, Kaufman Z, Sorek N, Brosh-Nissimov T. Delayed respiratory syncytial virus epidemic in children after relaxation of COVID-19 physical distancing measures, Ashdod, Israel, 2021. Euro Surveill. **2021**; 26(29).

11. CDC. Weekly U.S. Influenza Surveillance Report [Internet]. Centers for Disease Control and Prevention. 2022 [cited 2022 May 31]. Available from: https://www.cdc.gov/flu/weekly/weeklyarchives2021-2022/week17.htm

12. National flu and COVID-19 surveillance reports: 2021 to 2022 season [Internet]. GOV.UK. [cited 2022 May 31]. Available from: https://www.gov.uk/government/statistics/national-flu-and-covid-19-surveillance-reports-2021-to-2022-season

13. Stowe J, Tessier E, Zhao H, et al. Interactions between SARS-CoV-2 and influenza, and the impact of coinfection on disease severity: a test-negative design. Int J Epidemiol. **2021**; 50(4):1124–1133.

14. Xiang X, Wang Z-H, Ye L-L, et al. Co-infection of SARS-COV-2 and Influenza A Virus: A Case Series and Fast Review. Curr Med Sci. **2021**; 41(1):51–57.

15. Yue H, Zhang M, Xing L, et al. The epidemiology and clinical characteristics of co-infection of SARS-CoV-2 and influenza viruses in patients during COVID-19 outbreak. J Med Virol. **2020**; 92(11):2870–2873.

16. Ma S, Lai X, Chen Z, Tu S, Qin K. Clinical characteristics of critically ill patients co-infected with SARS-CoV-2 and the influenza virus in Wuhan, China. Int J Infect Dis. **2020**; 96:683–687.

17. Nickbakhsh S, Mair C, Matthews L, et al. Virus-virus interactions impact the population dynamics of influenza and the common cold. Proc Natl Acad Sci U S A. **2019**; :201911083.

18. Opatowski L, Baguelin M, Eggo RM. Influenza interaction with cocirculating pathogens and its impact on surveillance, pathogenesis, and epidemic profile: A key role for mathematical modelling. PLoS Pathog. **2018**; 14(2):e1006770.

19. Piret J, Boivin G. Viral Interference between Respiratory Viruses. Emerg Infect Dis. **2022**; 28(2):273–281.

20. Shinjoh M, Omoe K, Saito N, Matsuo N, Nerome K. In vitro growth profiles of respiratory syncytial virus in the presence of influenza virus. Acta Virol. **2000**; 44(2):91–97.

21. Pinky L, Dobrovolny HM. Coinfections of the Respiratory Tract: Viral Competition for Resources. PLoS One. **2016**; 11(5):e0155589.

22. Wu A, Mihaylova VT, Landry ML, Foxman EF. Interference between rhinovirus and influenza A virus: a clinical data analysis and experimental infection study. Lancet Microbe. **2020**; 1(6):e254–e262.

23. Dee K, Goldfarb DM, Haney J, et al. Human Rhinovirus Infection Blocks Severe Acute Respiratory Syndrome Coronavirus 2 Replication Within the Respiratory Epithelium: Implications for COVID-19 Epidemiology. J Infect Dis. **2021**; 224(1):31–38.

24. Cheemarla NR, Watkins TA, Mihaylova VT, et al. Dynamic innate immune response determines susceptibility to SARS-CoV-2 infection and early replication kinetics. J Exp Med. **2021**; 218(8):e20210583.

25. Essaidi-Laziosi M, Alvarez C, Puhach O, et al. Sequential infections with rhinovirus and influenza modulate the replicative capacity of SARS-CoV-2 in the upper respiratory tract. Emerg Microbes Infect. 11(1):412–423.

26. Vanderwall ER, Barrow KA, Rich LM, et al. Airway epithelial interferon response to SARS-CoV-2 is inferior to rhinovirus and heterologous rhinovirus infection suppresses SARS-CoV-2 replication. Sci Rep. **2022**; 12(1):6972.

27. Fage C, Hénaut M, Carbonneau J, Piret J, Boivin G. Influenza A(H1N1)pdm09 Virus but Not Respiratory Syncytial Virus Interferes with SARS-CoV-2 Replication during Sequential Infections in Human Nasal Epithelial Cells. Viruses. **2022**; 14(2):395.

28. Pizzorno A, Padey B, Julien T, et al. Characterization and Treatment of SARS-CoV-2 in Nasal and Bronchial Human Airway Epithelia. Cell Rep Med. **2020**; 1(4):100059.

29. Nicolas de Lamballerie C, Pizzorno A, Dubois J, et al. Characterization of cellular transcriptomic signatures induced by different respiratory viruses in human reconstituted airway epithelia. Sci Rep. **2019**; 9(1):11493.

30. Duchamp MB, Casalegno JS, Gillet Y, et al. Pandemic A(H1N1)2009 influenza virus detection by real time RT-PCR: is viral quantification useful? Clin Microbiol Infect. **2010**; 16(4):317–321.

31. Zlateva KT, Vijgen L, Dekeersmaeker N, Naranjo C, Van Ranst M. Subgroup Prevalence and Genotype Circulation Patterns of Human Respiratory Syncytial Virus in

Belgium during Ten Successive Epidemic Seasons. J Clin Microbiol. **2007**; 45(9):3022–3030.

32. Dubois J, Pizzorno A, Cavanagh M-H, et al. Strain-Dependent Impact of G and SH Deletions Provide New Insights for Live-Attenuated HMPV Vaccine Development. Vaccines (Basel). **2019**; 7(4).

33. Schibler M, Yerly S, Vieille G, et al. Critical Analysis of Rhinovirus RNA Load Quantification by Real-Time Reverse Transcription-PCR. J Clin Microbiol. **2012**; 50(9):2868–2872.

34. Nicolas De Lamballerie C, Pizzorno A, Dubois J, et al. Human Respiratory Syncytial Virus-Induced Immune Signature of Infection Revealed by Transcriptome Analysis of Clinical Pediatric Nasopharyngeal Swab Samples. J Infect Dis. **2021**; 223(6):1052–1061.

35. Hoffmann J, Machado D, Terrier O, et al. Viral and bacterial co-infection in severe pneumonia triggers innate immune responses and specifically enhances IP-10: a translational study. Sci Rep. **2016**; 6:38532.

36. Nicolas de Lamballerie C, Pizzorno A, Fouret J, et al. Transcriptional Profiling of Immune and Inflammatory Responses in the Context of SARS-CoV-2 Fungal Superinfection in a Human Airway Epithelial Model. Microorganisms. **2020**; 8(12):E1974.

37. Ruffin M, Bigot J, Calmel C, et al. Flagellin From Pseudomonas aeruginosa Modulates SARS-CoV-2 Infectivity in Cystic Fibrosis Airway Epithelial Cells by Increasing TMPRSS2 Expression. Front Immunol. **2021**; 12:714027.

38. Kim E-H, Nguyen T-Q, Casel MAB, et al. Coinfection with SARS-CoV-2 and Influenza A Virus Increases Disease Severity and Impairs Neutralizing Antibody and CD4+ T Cell Responses. J Virol. 96(6):e01873-21.

39. Zhang AJ, Lee AC-Y, Chan JF-W, et al. Coinfection by Severe Acute Respiratory Syndrome Coronavirus 2 and Influenza A(H1N1)pdm09 Virus Enhances the Severity of Pneumonia in Golden Syrian Hamsters. Clin Infect Dis. **2021**; 72(12):e978–e992.

FIGURES

Figure 1. Simultaneous infection with influenza virus and SARS-CoV-2. **A.** Nasal HAE were mock-infected or infected by influenza (H1N1) and/or SARS-CoV-2 at a MOI of 1 and incubated for 48h (n=3). Viral loads of SARS-CoV-2 and H1N1 were determined by RT-qPCR from total RNA extracted at 48hpi. **B.** Trans-Epithelial resistance (TEER ohms.cm2) was measured for all experimental conditions. **C/D.** Intracellular viral genome relative quantification by RTqPCR for SARS-CoV-2 (nsp14 gene) and influenza (M gene). **E.** Remodeling of the HAE ultrastructure during infection and co-infection by H1N1 and SARS-CoV-2. a) Regular ultrastructure of mock-infected nasal reconstituted human airway epithelia; b-d) MucilAir™ HAE were infected on the apical surface with SARS-CoV-2 (b), or H1N1 (c) or co-infected with both viruses (d). At 48 hpi, HAE were fixed and processed for transmission electron microscopy analysis, as described in Materials and Methods. Section of SARS-CoV-2 infected cells (*) showing numerous viral vesicles (DMVs) and H1N1-infected cells (#) showing numerous M1-associated rod-like structures (arrowhead) accumulated within the nucleoplasm. N: nucleus, Nu: nucleolus, V: viral particles.

Figure 2. Influenza/SARS-CoV-2 mutual superinfections. A. Nasal HAE were mock-infected or infected by influenza (H1N1) or SARS-CoV-2 at a MOI of 0.1 and were superinfected at 48hpi by the other virus (MOI 0.1) and incubated for another 48h. **B.** Trans-Epithelial resistance (TEER ohms.cm2) was measured for all experimental conditions. **C.** Apical or **D.** Intracellular viral genome relative quantification by RTqPCR for SARS-CoV-2 (nsp14 gene) and influenza (M gene). **E.** Differential expression of both immune response (96 genes) and type III IFNs (12 genes) panels were evaluated in infected nasal HAE using the Nanostring technology. Heatmap and hierarchical clustering (one minus pearson correlation)

of differentially expressed genes compared to mock condition. Genes of interest in the text are highlighted with orange and green boxes.

Figure 3. SARS-CoV-2 superinfection in the context of influenza, RSV, hMPV, or hRV prior infections. A. Nasal HAE were mock-infected or infected by influenza (H1N1) or RSV, hMPV or hRV at a MOI of 0.01, 0.1, 1 and 5, respectively and incubated for seven days (T7dpi), and then superinfected by SARS-CoV-2 (MOI 0.1) for 2 additional days. **B.** Trans-Epithelial resistance (TEER ohms.cm2) was measured for all experimental conditions. **C.** Intracellular viral genome relative quantification by RTqPCR for influenza (M gene), RSV (F gene), hMPV (N gene) or hRV (N gene) **D.** Intracellular viral genome relative quantification by RTqPCR for SARS-CoV-2 (nsp14 gene).

Figure 4. Immune response of SARS-CoV-2 superinfection in the context of influenza, RSV, hMPV or hRV prior infections. Differential expression of both immune response (96 genes) and type III IFNs (12 genes) panels were evaluated in infected nasal HAE using the Nanostring technology. Heatmap and hierarchical clustering (one minus pearson correlation) of differentially expressed genes in the context of superinfection compared to primary infection. Genes of interest in the text are highlighted with yellow, orange and green boxes.

Supplementary Figure 1. Immune response of SARS-CoV-2 superinfection and influenza, RSV, hMPV or hRV primary infections. Differential expression of both immune response (96 genes) and type III IFNs (12 genes) panels were evaluated in infected nasal HAE using the Nanostring technology. Heatmap and hierarchical clustering of differentially expressed genes compared to mock condition.

Virus	Viral strain	Target	Primers/probes
SARS-CoV-2	BetaCoV/France/IDF0571/2020	Nsp14 [28]	Forward 5'-TGGGGYTTTACRGGTAACCT-3'
			Reverse 5'-AACRCGCTTAACAAAGCACTC-3'
			Probe 5'-FAM-TAGTTGTGATGCWATCATGACTAG-TAMRA-3'
Influenza	A/Lyon/969/2009(H1N1)	M [30]	Forward 5'-CTTCTAACCGAGGTCGAAACGTA-3'
			Reverse 5'-GGTGACAGGATTGGTCTTGTCTTTA-3'
			Probe 5'-TCAGGCCCCCTCAAAGCCGAG-3'
RSV	hRSV-A Long strain ATCC-VR26	F [31]	Forward 5'-CTGTGATAGARTTCCAACAAAAGAACA-3'
			Reverse 5'-AGTTACACCTGCATTAACACTAAATCC-3'
			Probe 5' FAM-CAGACTACTAGAGATTAC-3'
hMPV	hMPV-B strain CAN97-82 (B1)	N [32]	Forward 5'-AGAGTCTCAGTACACAATAAAAAGAGATGTGGG-3'
			Reverse 5'-CCTATTTCTGCAGCATATTTGTAATCAG-3'
hRV	hRV-A16 ATCC VR-283	5'UTR [33]	Forward 5' AGCCTGCGTGCCKGCC 3'
			Reverse 5' GAAACACGGACACCCAAAGTAGT 3'
			Probe 5' FAM-CTCCGGCCCCTGAATGYGGCTAA-TAMRA 3'

Table 1. List of primer & probes used in this study

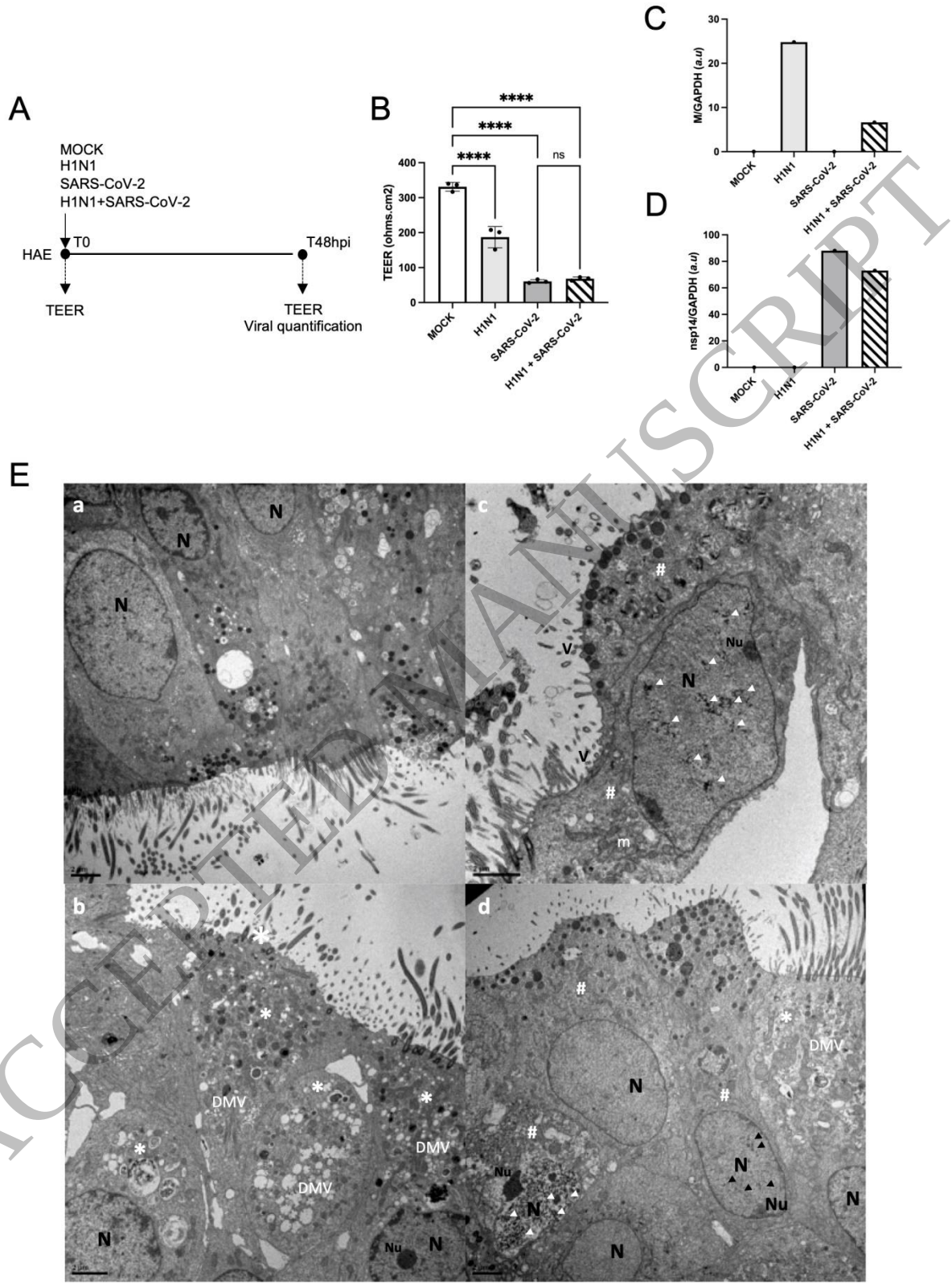

Figure 1

Figure 1
387x559 mm (79 x DPI)

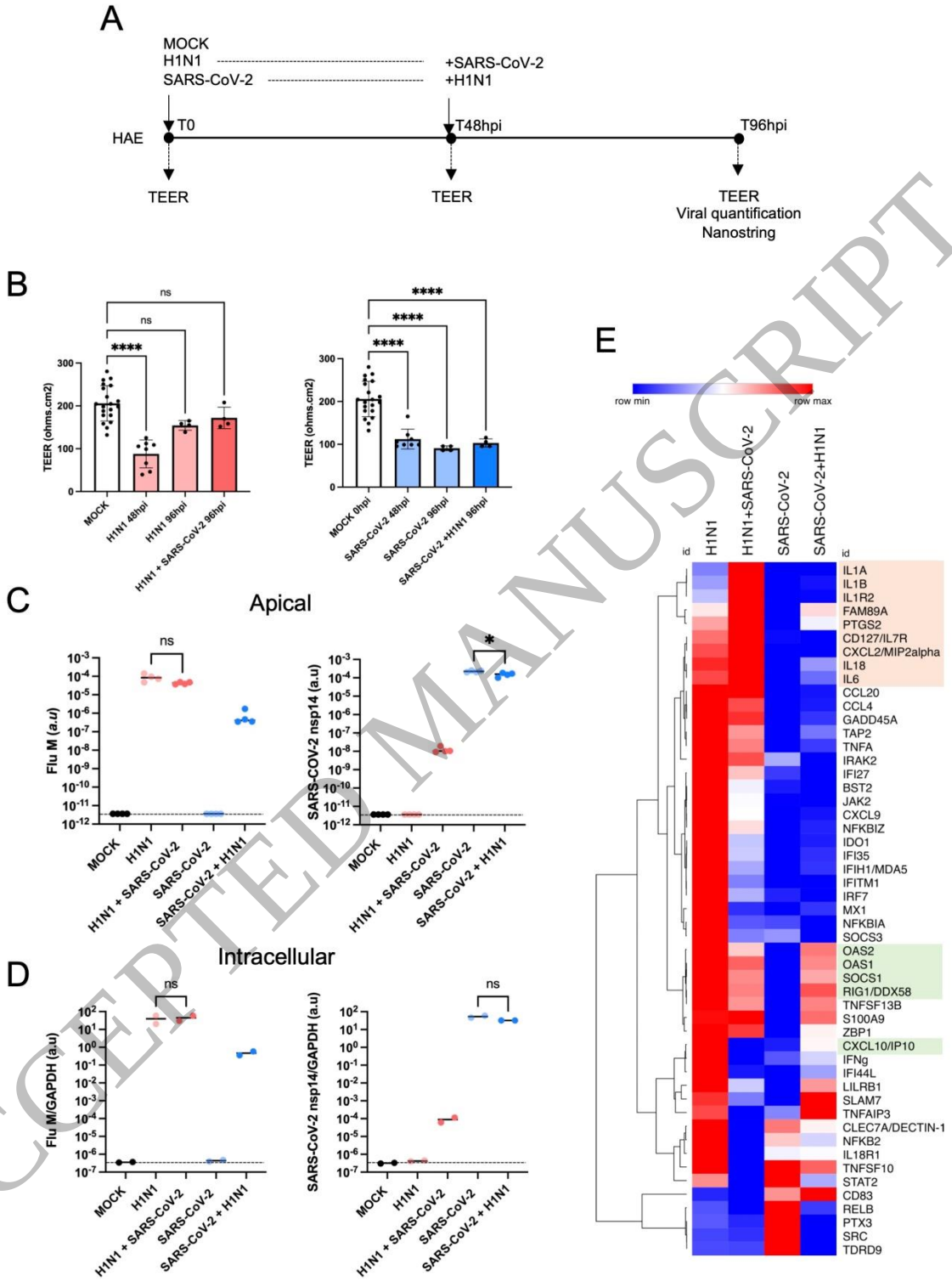

Figure 2

Figure 2
190x275 mm (79 x DPI)

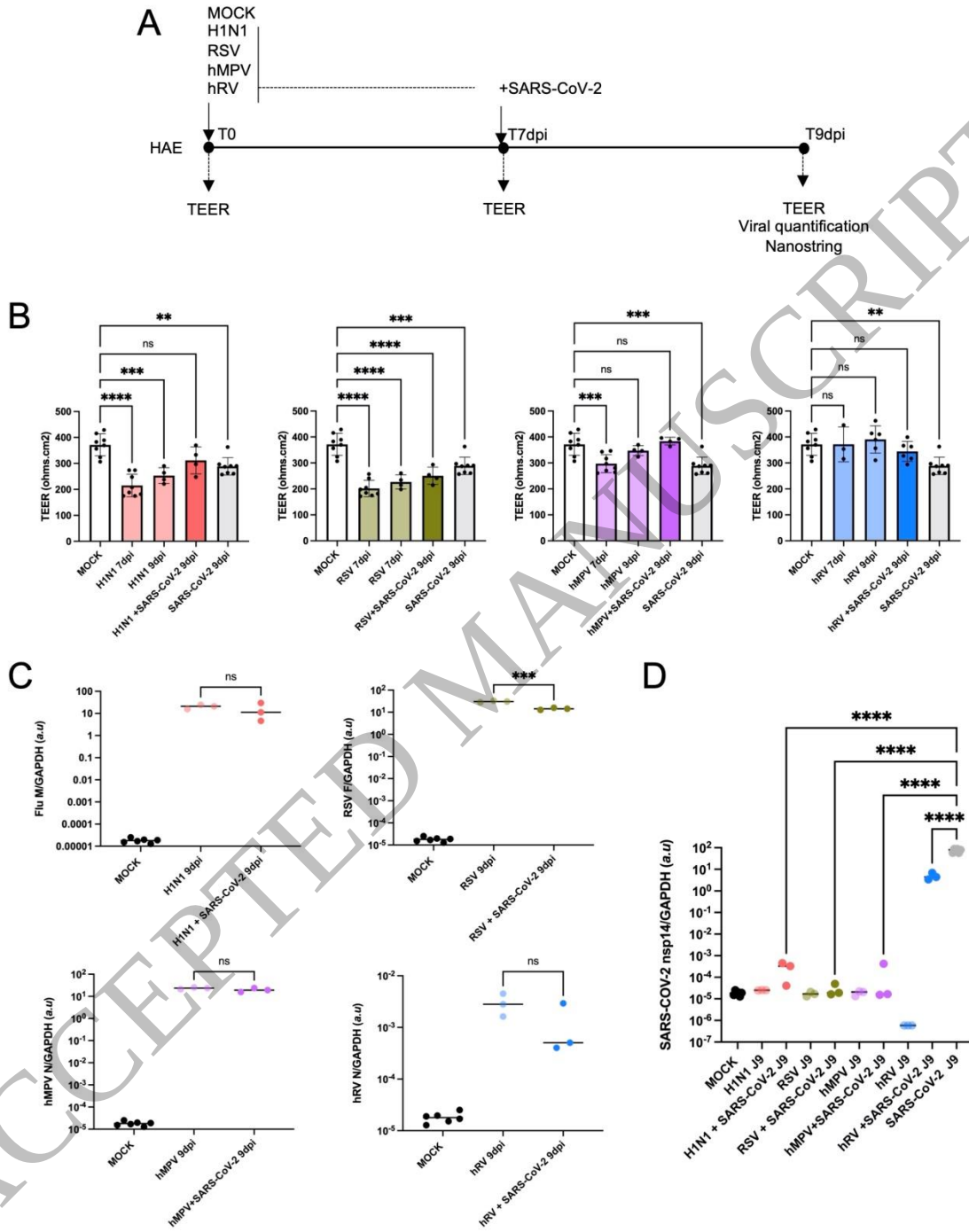

Figure 3

Figure 3
190x275 mm (79 x DPI)

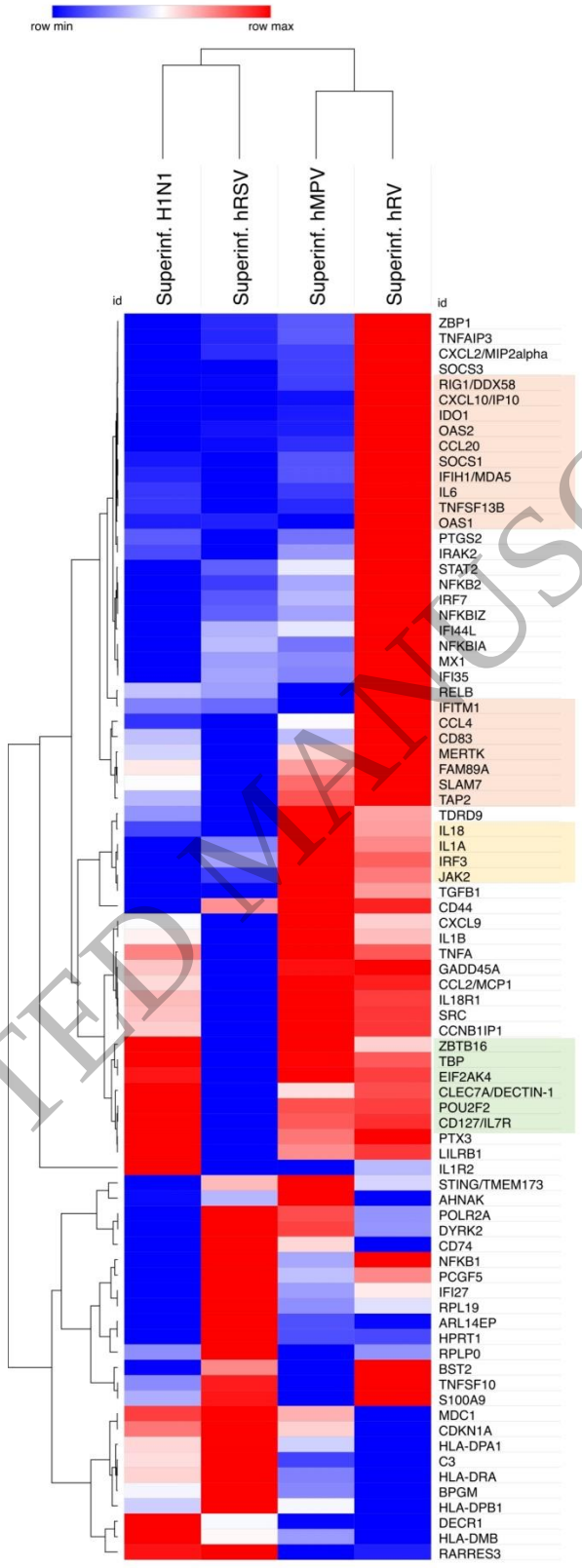

Figure 4

Figure 4
190x275 mm (79 x DPI)